https://doi.org/10.5194/essd-2026-218
Preprint. Discussion started: 22 April 2026

Open Access Earth System Science Data Discussions

Global and National CO_2 Emission from Lime Production Process and Carbonation sink from 1930 to 2024

Longfei Bing[1,3,4#], Xiaoyu Zhang[1,5#], Le Niu[1,5], Jiaoyue Wang[1,3,4*], Jiajie Li[2], Xue Jiang[2], Fengming, Xi[1,2,3,4*]

1 Key Laboratory of Forest Ecology and Silviculture, Institute of Applied Ecology, Chinese Academy of Sciences, Shenyang 11001, China

2 Institute of Mineral Resources, University of Science and Technology Beijing, Beijing, 100083, China

3 Key Laboratory of Terrestrial Ecosystem Carbon Neutrality, Shenyang 110016, China

4 National-Local Joint Engineering Laboratory of Contaminated Soil Remediation by Bio-physicochemical Synergistic Process, Shenyang 110016, China

5 University of Chinese Academy of Sciences, Beijing 100049, China

# These authors contributed equally to this work.

*Correspondence to: Fengming Xi(xifengming@ustb.edu.cn); Jiaoyue Wang (wangjiaoyue@iae.ac.cn)

Abstract

Accurate quantification of both lime process emissions and carbonation sink is essential for the Global Carbon Budget (GCB). By extending temporal coverage (1930–2024), refining spatial resolution (11 major lime-producing countries), and expanding system boundaries (adding Blast Furnace Slag, BFS), this study constructs the first standardized dataset of lime CO_2 process emissions and carbonation sink covering 81.09% of global lime production. We estimate cumulative global lime process emissions are 15.29 Gt CO_2 (95% CI: 13.81–16.79 Gt CO_2), with the construction and metallurgical sectors serving as primary sources, contributing 5.80 Gt CO_2 (37.92%) and 5.04 Gt CO_2 (32.95%), respectively. During the same period, cumulative lime carbonation sink reached 7.33 Gt CO_2 (95% CI: 5.95–8.88 Gt CO_2), achieving a carbon offset ratio (cement carbonation sink to process emission) of 47.65%, which is 8.32% increase compared with Bing et al. (2023). The lime carbonation sink in 2024 accounted for approximately 1.5%–2% of the global terrestrial carbon sink in 2023. China is the main contributor, with cumulative emissions of 8.89 Gt CO_2 (58.13% of the global total) and cumulative carbonation sink of 4.21 Gt CO_2 (57.45% globally) from 1930 to 2024. Lime-stabilized soil (LSS, 36.53 %), mortar (MOR, 18.66 %), steel slag (SS, 17.73 %), and blast furnace slag (BFS, 12.83 %) were the primary carbon uptake materials, collectively accounting for 85.75 % of the total carbonation sink. Significant regional disparities were

https://doi.org/10.5194/essd-2026-218
Preprint. Discussion started: 22 April 2026

Open Access Earth System Science Data Discussions

pronounced: developed countries (e.g., those in Europe, the United States, Japan, and Australia) have already peaked in lime process carbon emissions, with net emissions gradually approaching zero. In contrast, developing countries such as China and Brazil continue to exhibit growth in both emissions and carbonation sink. Although their carbon-offset levels exceed 50%, they face substantial pressure to reduce total emissions. This dataset provides critical data for incorporating the lime carbonation sink into the Global Carbon Budget. It also contributes to optimizing global carbon modelling and regional carbon-neutrality pathways. The dataset is archived on Zendo https://doi.org/10.5281/zenodo.18616060 (Bing et al., 2026)

1. Introduction

Lime serves as an indispensable feedstock in numerous industrial processes, playing a pivotal role in sectors such as steelmaking, construction materials, chemical engineering, and wastewater treatment (Revuelta, 2021). Over the past two decades, driven by urbanization, industrialization, and the rapid development of large-scale infrastructure, global lime production has surged by 3.4-fold, increasing from 121 Mt in 2004 to 420 Mt in 2024 (USGS, 2026a). Projections indicate that two-thirds of the global population will reside in urban areas by 2050 (UN-Habitat, 2022). This ongoing urbanization process is expected to further drive the demand for housing, transportation infrastructure, and environmental sanitation facilities, thereby leading to sustained increase in the consumption of lime as a fundamental material.

Characterized by high carbon intensity, the lime industry is one of the major sources of greenhouse gas emissions in the Industrial Processes and Product Use (IPPU) sector, ranking third after the cement and steel industries (IPCC, 2006). Approximately 65% of global CO_2 emissions originates from the calcination of limestone (Han et al., 2022). While the remaining 35% of CO_2 emissions is attributed to fossil fuel combustion and electricity consumption (Laveglia et al., 2024a). Unlike the energy sector, the CO_2 emissions in lime production process are dictated by chemical reactions and cannot be fully eliminated through fuel switching or energy efficiency improvements. Consequently, the lime industry is a quintessential "hard-to-abate" industrial sector (Davis et al., 2018). Quantifying the CO_2 emissions from lime production process is of great significance for CO_2 management and global carbon budget.

However, accurately quantifying process emissions from the global lime industry remains a significant challenge, primarily due to data gaps and inconsistent statistical frameworks. First, large volumes of lime are produced for internal use by steel, sugar, and chemical enterprises, which does not enter commercial circulation. The prevalence of this "captive production" leads to omit much of the output and severely underestimate the official activity data (USGS, 2026a). Second, significant disparities in kiln technology exist across regions. The coexistence of traditional vertical kilns in developing countries and high-efficiency rotary kilns in developed countries leads to substantial fluctuations in emission factors (European Commission, 2013). As Robbie Andrew noted in studies of global process emissions, the accuracy of emission factors depends heavily on precise raw material composition (Andrew, 2019). Ignoring these variations results in significant process emissions estimation biases. Furthermore, overlapping statistical boundaries between lime and cement production often lead to misclassification or omissions in historical data, which making it is difficult for existing databases to reflect the true

https://doi.org/10.5194/essd-2026-218
Preprint. Discussion started: 22 April 2026

Open Access Earth System Science Data Discussions

emission trajectory of lime industry (Andrew, 2019). According to the China Building Materials Federation, total CO_2 emissions from China's building materials industry reached 1.48 billion tons in 2020, representing 14.9% of the national total, with the lime sector contributing approximately 8.1% of the industry's emissions (CBMEMA, 2026). Globally, the lime industry contributes approximately 1% of total anthropogenic CO_2 emissions (Campo et al., 2021; Bridlington et al., 2022). Notably, lime is extensively utilized in iron and steel, construction, chemical engineering, agriculture, and environmental remediation (European Commission, 2013). During their lifecycle, lime-based materials undergo carbonation with atmospheric CO_2 via Eqs. (1) and (2), thereby sequestering a portion of the process CO_2 released by their production (Simoni et al., 2022). Previous study revealed that between 1930 and 2020, global lime materials cumulatively sequestered approximately 144.47 Mt C (95% CI: 101.62–196.11 Mt C), offsetting 38.83% of process emissions over the same period (Bing et al., 2023).

$$CaO + H_2O = Ca(OH)_2 \quad \text{Eq (1)}$$

$$Ca(OH)_2 + CO_2 = CaCO_3 + H_2O \quad \text{Eq (2)}$$

Carbonation represents a pivotal pathway for achieving net-zero emissions in the lime industry. Although previous studies have indicated that CO_2 emissions from lime production can be mitigated by substituting fossil fuels with residue-derived fuels (Zementwerke eV, 2021), replacing calcium carbonate calcination with electrochemical (Ellis et al., 2020), and chemical decarbonization methods (Hanein et al., 2021), these approaches are currently constrained by high costs and technical complexities and making challenges in large-scale deployment (Simoni et al., 2022). Consequently, carbon sequestration via lime carbonation plays an alternative role in the decarbonation of the sector, which creating an urgent need to accurately quantify its contribution. Currently, China's Action Plan for Carbon Peaking by 2030 in the Building Materials Industry promotes utilization of industrial solid wastes, such as steel slag and carbide slag (MIIT, 2026). Similarly, the European Lime Association explicitly identifies Carbon Capture, Utilization, and Storage (CCUS) and natural carbonation as critical measures, aiming to achieve CO_2 negative emissions by 2050 through technological upgrades (EuLA, 2026a). The National Lime Association (NLA, 2023) in the United States also released a roadmap targeting carbon neutrality by 2050, emphasizing the significance of the carbon sink function of lime products. At present, the Global Carbon Budget (GCB) has incorporated cement carbonation sink into the anthropogenic CO_2 sink (Friedlingstein et al., 2022). However, the lime carbonation sink remains excluded. For context, carbon uptake by cement materials in 2021 accounted for approximately 8.23% of the global mean land carbon sink from 2010–2020 (Huang et al., 2023; Friedlingstein et al., 2020), whereas lime materials sequestered an amount equivalent to approximately 1.09% of the mean land sink from 2012–2020 (Bing et al., 2023). Incorporating the lime carbonation sink into the GCB would provide a more accurate reflection of the global carbon cycle and optimize regional carbon budget allocations. Therefore, an accurate accounting of lime carbonation sink is indispensable.

Previous efforts by our team provided a preliminary accounting of lime-based carbonation sink in China and the United States (Bing et al., 2023). However, the study treated the rest of the world as a homogeneous entity. It overlooks the significant divergence in process carbon emissions and sequestration coefficients caused by variations in production technologies, raw material compositions, and application industries across different nations. In particular, the

https://doi.org/10.5194/essd-2026-218
Preprint. Discussion started: 22 April 2026

carbon sequestration of metallurgical wastes has been historically underestimated. For instance, pig iron production requires the addition of quicklime and limestone as metallurgical fluxes (Yang et al., 2024). The resulting slag, with calcium oxide (CaO) content ranging from 30% to 50% (Ren et al., 2021), presents substantial carbon sequestration (Gomari et al., 2024), which is also one of key improvements of this study. Furthermore, global production rates of iron and steel slag have generally declined due to optimized furnace lining materials and refined blowing processes (Naito et al., 2015). Concurrently, the resource utilization of these materials has continued to improve. On a global scale, blast furnace slag (BFS) and steel slag (SS) are widely repurposed for cement production, road construction, building materials, and fertilizers (Heraiz et al., 2025). However, significant disparities exist at the national level. The developed nations have achieved comprehensive utilization rates of steel slag exceeding 90%, while the rate in China remains approximately 20% (Gao et al., 2023). By accounting for these technological and regional discrepancies, this study provides a more robust quantification of the global lime process emissions and carbonation sink.

To address the challenges of global lime process emissions accounting and facilitate the integration of lime carbonation sink into the GCB dataset, this study significantly expands the data framework through the following improvements. (1) Spatiotemporal Reconstruction and Verification of Activity Data. To bridge the statistical gaps caused by "captive production," the accounting scope was extended to 11 major lime-producing countries, covering 87.62% of global output. The United States Geological Survey (USGS) mineral statistics (USGS, 2026a) complemented by national lime association reports and statistical yearbooks were used (SI-2 Data1). Cross-verification was performed to correct systemic omissions in official statistics. Furthermore, the temporal scope was extended to 1930–2024 to synchronize with the Global Carbon Budget timeframe. (2) Localized Refinement of Lime Emission Factors. Following the "localized emission factor" methodology proposed by (Liu et al., 2015), emission factors was adjusted based on specific calcium oxide (CaO) content requirements across downstream sectors, such as the high-purity demands of the metallurgical industry. By integrating these standards with sector-specific consumption ratios, lime emission factors were back-calculated, a refinement that substantially reduces uncertainty in process emissions accounting. (3) Integration of Lime Materials within Blast Furnace Slag (BFS). By recognizing that BFS contains lime-based components with carbonation potential similar to steel slag, BFS was formally incorporated into the accounting boundary. This inclusion ensures a more comprehensive quantification of the global lime-related carbonation sink. (4) Dynamic Parameterization of Technological Evolution. Through accounting for regional variations in iron and steel industry and the global diversity of slag disposal environments, dynamic accounting parameters were implemented. Specifically, a tiered temporal approach was applied to reflect changes in slag production and utilization rates, which divided into 1930–1950 (wartime catalysts and industrial shifts), 1950–1970 (efficiency revolution and process standardization), 1970–2000 (energy crises and technological optimization), and 2000–2024 (green development and intelligent manufacturing). Unlike previous studies that assumed static values, this multi-period setting captures the 20-to-30-year generational cycles of metallurgical technology, which could more accurately reflecting the impacts of technical progress on the lime process emissions estimation and carbon sequestration potential of lime materials

https://doi.org/10.5194/essd-2026-218
Preprint. Discussion started: 22 April 2026

embedded in slag. These improvements enhance the precision of global lime industry emission inventories by correcting foundational data and refining emission parameters. Simultaneously, the reduction in accounting uncertainties stemming from regional disparities and technological transitions, providing a robust parametric foundation for independent national carbon assessments.

2. Data Sources and Methodology

2.1. Data Sources and Processing

The dataset constructed in this study spans the period from 1930 to 2024, covering 11 major lime-producing nations (China, The United States of America, The United Kingdom, France, Germany, Italy, Australia, Canada, Brazil, Japan, and Russia) as well as the "Rest of the World" (ROW).

2.1.1. Core Basic Data

(1) Lime Production Data

1930–2020: Data for China and the USA were adopted from the verified dataset established by (Bing et al., 2023), while production data for 2021–2024 were sourced from the United States Geological Survey (USGS).

1930–1958: Lime production data for Japan (Shimanish, 2004), Brazil (IBGE, 2026), France (ASF, 2026), and Canada (Dominion Bureau of Statistics, 2026) were derived from historical literature and statistical yearbooks. For Italy and Germany, production figures were estimated using multiple linear regression models; the detailed regression coefficients are provided in Supplementary Table SI-2 Data1. For Australia, lime production was calculated based on the proportion of limestone allocated for lime manufacturing and the limestone-to-lime conversion rate, with underlying limestone production data obtained from the *Year Book Australia* (ABS, 2026). For the United Kingdom, lime production was estimated based on limestone and dolomite production figures, utilizing specific allocation ratios for lime production (0.161 and 0.049, respectively) and an average lime yield factor of 0.225 (Ordnance Survey, 2026). Russian lime production data were sourced from the *Statistical Yearbook of the USSR* (1961), with data for missing years filled using linear interpolation.

1959–2024: Data for the 11 countries were sourced from the United States Geological Survey (USGS). Notably, data for Russia from 1959 to 1991 were derived by multiplying the total lime production of the Soviet Union by Russia's average share (0.54); this proportion was obtained from the Statistical Yearbook of the National Economy of the USSR (1961) (Upravlenie S. U. T. statisticheskoe, 1961). Detailed datasets are provided in Supplementary Table SI-2 Data 1.

(2) Industrial Product Output Data

For the period from 1930 to 2020, data on crude steel, alumina, and paper and paperboard for China, the United States, and the global total were adopted from the verified dataset constructed by (Bing et al., 2023). For 2021–2024, data on crude steel and alumina for China, the United States, additional countries, and the global total were sourced from the USGS, while data on paper and paperboard were obtained from the *FAO Yearbook of Forest Products*. Specific data sources were organized as follows:

Crude steel and pig iron: Data for additional countries from 1959 to 2024 were retrieved from the *USGS Iron and Steel Slag Database* (USGS, 2026b), while historical data from 1930

https://doi.org/10.5194/essd-2026-218
Preprint. Discussion started: 22 April 2026

to 1958 were sourced from the British Geological Survey (BGS, 2026.). Detailed datasets are provided in Supplementary Table SI-2 Data 2 and Data3.

Alumina: Data for additional countries covering 1959–2024 were obtained from the USGS Bauxite and Alumina Database (USGS, 2026c). Data for the 1930–1958 period were derived from the British Geological Survey (BGS, 2026) and the *Statistical Yearbook of France* (ASF, 2026). Detailed datasets are provided in Supplementary Table SI-2 Data 4.

Paper and paperboard: Data from 1946 to 2024 were sourced from the FAO Yearbook of Forest Products (FAO, 2026), and data from 1930 to 1945 were obtained from the *United Nations Statistical Yearbook* (UNSDW, 2026). Detailed datasets are provided in Supplementary Table SI-2 Data 5.

2.1.2. Key Calculation Parameters

(1) Carbon Emission Factors

Carbon emission factors (CEF) were determined following the "Tier 2" approach outlined in the 2006 IPCC Guidelines for National Greenhouse Gas Inventories (IPCC, 2026), based on the CaO content of different lime types. Specifically, the CEFs for the United States, China, the UK, France, Germany, Italy, Japan, Canada, Brazil, Russia, Australia, and other countries were calculated as 0.742, 0.716, 0.732, 0.728, 0.733, 0.733, 0.728, 0.741, 0.737, 0.733, 0.729, and 0.737 t CO_2/t lime, respectively. Detailed literature sources are provided in Supplementary Table SI-3 Data 1.

(2) Carbonation-related parameters

CaO Content: Data on the CaO content of materials—including Steel Slag (SS), Blast Furnace Slag (BFS), red mud (RM), and lime mud (LM)—were obtained through a systematic review of the literatures and reports from industry associations (e.g., the European Lime Association (EuLA,2026b), Detailed literature sources are provided in Supplementary Table SI-3 Data 7.

The carbonation ratio (γ) is defined as the proportion of calcium oxide converted to calcium carbonate. For Precipitated Calcium Carbonate (PCC) and Carbonation Sugar (SUG), γ was set to 1, indicating complete carbonation during the production process (Wang and Shen, 2002). For Lime-Stabilized Soil (LSS), carbide slag (CS), and Lime Kiln Dust (LKD), the annual carbonation ratio (R) was assumed to be 1, representing complete carbonation within one year. Based on the specific disposal or stacking scenarios, different kinetic models were applied. The slab model (Wu et al., 2024) was used to describe the carbonation process of lime mortar (Fig. 1); the pile model (Xi et al., 2016) was adopted to simulate the carbonation of lime mud and red mud; and the spherical model (Manocha and Ponchon, 2018) was employed for SS and BFS.

https://doi.org/10.5194/essd-2026-218
Preprint. Discussion started: 22 April 2026

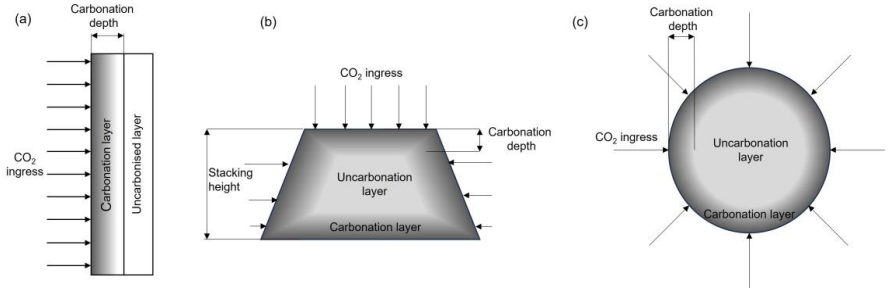

Fig. 1. Schematic diagrams of the carbonation models: (a) the slab model for lime mortar; (b) the pile model for paper lime mud and red mud; and (c) the spherical model for iron and steel slag.

(3) Industrial and Technological Parameters

Lime utilization share, the proportion of lime used across different sectors specifically construction (LSS + MOR), metallurgy (SS + BFS + RM), and the chemical industry (PCC + CS + SUG + LM) was determined for different countries based on the literatures. Detailed literature sources are provided in Supplementary Table SI-3 Data 3-6. For generation and utilization rates of SS and BFS, the parameters were established by reviewing country-specific literatures. Based on the technological evolution of the iron and steel industry (Naito et al., 2015), the timeline was divided into four distinct phases: 1930–1950, 1950–1970, 1970–2000, and 2000–2024. Detailed literature sources are provided in Supplementary Table SI-3 Data 9.

2.2. Estimation of Process CO_2 Emissions from Lime Production

Calculations were conducted using the Tier 2 method from the 2006 IPCC Guidelines for National Greenhouse Gas Inventories (IPCC, 2006), considering CO_2 emissions generated solely from limestone calcination. The calculation formula is as follows:

$$E_{progress,i} = P_{lime,i} \times EF_{lime,i} \quad (3)$$

where, $E_{progress,i}$ represents the industrial process CO_2 emissions from the lime industry in country i; $P_{lime,i}$ denotes the annual lime production of country i; $EF_{lime,i}$ is the CO_2 emission factor for lime production in country i.

2.3. Estimation of CO_2 Uptake by Lime

The system boundary, established via Material Flow Analysis (MFA), encompasses ten categories of lime-based materials classified by their lifecycle stages. Specifically, LKD is categorized as a direct by product of the lime production process. Beyond the production stage, nine industrial byproducts and materials are incorporated across three sectors: metallurgy (SS, BFS, RM), chemicals (PCC, CS, SUG, LM), and construction (LSS, MOR). Notably, BFS is newly integrated to rectify previous accounting omissions in the metallurgical carbonation sink.

2.3.1. General Calculation Model

(1) Carbon Sequestration

Based on the stoichiometry of the calcium oxide carbonation reaction, the governing equations for all materials were established by incorporating material production, CaO content, conversion efficiency, and carbonation ratio. The carbon sequestration (CO_2) is calculated as follows:

$$C = M \times f^{CaO} \times \gamma \times R \times \frac{M_{CO_2}}{M_{CaO}} \quad \text{Eq (4)}$$

https://doi.org/10.5194/essd-2026-218
Preprint. Discussion started: 22 April 2026

Open Access Earth System Science Data Discussions

where, M represents the production volume of lime materials; f^{CaO} denotes the mass fraction of CaO in the material (%); and γ signifies the conversion rate of CaO to $CaCO_3$, which is assumed to be 100% for PCC and SUG, while specific values for other materials are detailed in Supplementary Table SI-3 Data 1. The variable R indicates the annual carbonation rate (%); specifically, R is set to 1 for materials capable of complete carbonation within a single year (i.e., LKD, LSS, CS, PCC, and SUG), whereas for materials that do not fully carbonate within one year (i.e., MOR, LM, RM, SS, and BFS), R is calculated using distinct models tailored to each material type (see Supplementary Table SI-3 Data10). Finally, $\frac{M_{CO2}}{M_{CaO}}$ represents the molar mass ratio of carbon to calcium oxide (44/56).

(2) Annual Carbonation Ratio

The carbonation process of lime-based materials was simulated using three geometric models, including the slab model, the pile model, and the spherical model.

For the slab model, the annual carbonation ratio R_{lime} is expressed as:

$$R_{lime} = \left(d_{lime,i} - d_{lime,i-1}\right)/d_T \quad \text{Eq (5)}$$

where, $d_{lime,i}$ denotes the carbonation depth of lime-based materials (such as MOR) in year i, while d_T signifies the design thickness of lime.

In the pile model, the annual carbonation ratio R_{lime} is defined as:

$$\mathrm{R_{lime,i}} = \begin{cases} \frac{k_{mud}\times\sqrt{t_i}}{\frac{h_{mud}}{t_{mud}}\times t_i}\,(t_i \le t_{lm}), \\ \frac{d_{mud,i}}{h_{mud}}\,(t_{mud} < t_i < 100), \end{cases} \quad \text{Eq (6)}$$

where, $R_{lime,i}$ signifies the carbonation ratio in the i-th year, d_{mud} is the carbonation depth calculated using the carbonation rate k_{mud} and time t_i, $d_{mud,i} = k_{mud} \times \left(\sqrt{t_i} - \sqrt{t_{i-1}}\right)$, while h_{mud} and t_{mud} represent the stacking height and storage duration of the lime-based material, respectively.

In the spherical model, the annual carbon uptake ratio R_{lime} is expressed as:

$$R_{lime,i} = \begin{cases} 100\% - \frac{\int_a^b \frac{\pi}{6}(D-D_{slag})^3}{\int_a^b \frac{\pi}{6}D^3} \times 100\% & (a > D_{slag}) \\ 100\% - \frac{\int_{D_0}^b \frac{\pi}{6}(D-D_{slag})^3}{\int_a^b \frac{\pi}{6}D^3} \times 100\% & (a \le D_{slag} \le b) \\ 100\% & (b < D_{slag}) \end{cases} \quad \text{Eq (7)}$$

Where, D denotes the particle size of the slag; D_{slag} represents the maximum diameter of completely carbonated slag lumps (SS or BFS); a and b stand for the corresponding minimum and maximum particle sizes of slag particles in a given particle size distribution; $D_{slag} = 2d_{slag,i} = 2k_{slag} \times \sqrt{t_i}$, $d_{slag,i}$ is the carbonation depth of the slag in the i-th year, k_{slag} refers to the carbonation rate of the slag, and t_i denotes the carbonation duration.

(3) Calculation of Annual and Cumulative Uptake

The carbon uptake from the multi-year carbonation of BFS, SS, Red Mud, and Carbide Slag is calculated by multiplying the annual carbonation ratio by the solid waste mass. Regional totals are obtained by summing the uptake across all lime-based materials. Additionally, the annual CO_2 uptake for the t_i th year is defined as the increment in cumulative uptake from year t_{i-1} to t_i, calculated using Equation (8). This quantifies the annual contribution of lime materials

https://doi.org/10.5194/essd-2026-218
Preprint. Discussion started: 22 April 2026

to the total carbon sink.

$$\Delta C_{lime,total}^{t_i} = \sum C_{lime,total}^{t_i} - \sum C_{lime,total}^{t_{i-1}} \quad \text{Eq (8)}$$

Where, $\Delta C_{lime,total}^{t_i}$ denotes the carbon uptake in the *i*-th year, $\sum C_{lime,total}^{t_i}$ represents the cumulative carbon uptake to the *i*-th year, and $\sum C_{lime,total}^{t_{i-1}}$ is the cumulative carbon uptake to the (i−1)-th year.

2.3.2 Details of Material-Specific Calculations

(1) Lime materials from the production progress (LKD)

LKD is a byproduct of lime calcination. Its production is calculated as $M_{lkd} = m_{lime} \times r_{lkd}$, where r_{lkd} represents the industry default generation rate of kiln dust. Due to its fine particle size and high specific surface area, LKD undergoes rapid carbonation during stockpiling; therefore, the carbonation ratio is assumed to be $R_{lkd} = 100\%$.

(2) Lime Materials in the Construction Industry (LSS, MOR)

For LSS, $M_{lss} = m_{lime} \times L_1 \times a_1$, where L_1 represents the proportion of lime utilized in the construction sector, and a_1 denotes the share of lime allocated to LSS within the construction sector.

For MOR, $M_{mor} = m_{lime} \times L_1 \times a_2$, where a_2 denotes the proportion of lime allocated to MOR within the construction sector. The slab model was adopted to calculate the carbonation ratio R_{mor}, as expressed in the following equation: $R_{mor} = \frac{d_{mor,i} - d_{mor,i-1}}{d_T}$, where d_T represents the design thickness of the mortar, and $d_{mor,i}$ denotes the carbonation depth in the i-th year. Based on Fick's laws of diffusion, the carbonation depth is calculated as $d_{mor} = k_{mor} \times \sqrt{t_{mor}}$, where k_{mor} is the carbonation rate coefficient of MOR, and t_{mor} represents the duration of carbonation.

(3) Lime Materials in the Metallurgical Industry (SS, BFS, RM)

For SS, The production of SS is strongly correlated with crude steel output $(m_{crude\,steel})$. The mass is calculated as: $M_{ss} = m_{crude\,steel} \times r_{ss} \times U_{ss}$, where r_{ss} represents the steel slag generation rate (time-dependent values are provided in SI-3 Data 1), and U_{ss} denotes the ratio of stockpiling or roadbed utilization. The carbonation process was approximated using the uniform spherical model proposed by Bing et al. (2023), as shown in Equation (7).

For BFS, $M_{bfs} = m_{bfs,} \times r_{bfs} \times l_{bfs} \times U_{bfs}$, where, r_{bfs} is the generation rate of blast furnace slag (time-dependent values, see SI-3 Data 1); l_{bfs} represents the proportion of CaO in the slag derived specifically from lime; and U_{bfs} denotes the stockpiling/utilization ratio, following the same logic as SS. The carbonation model is consistent with that of SS (spherical model, Equation 7).

For RM, $M_{rm} = m_{alumina} \times r_{rm} \times (1 - U_{rm})$, where, r_{rm} is the red mud generation rate, and U_{rm} is the comprehensive utilization rate of red mud. The carbonation ratio was calculated using the pile model (Equation 6). Based on the average storage duration in red mud yards and the laboratory-measured carbonation rate k_{rm}, the carbon sequestration was quantified cumulatively on an annual basis.

(4) Lime Materials in the Chemical Industry (PCC, SUG, CS, LM)

For PCC and SUG, $M_{pcc} = m_{lime} \times L_2 \times b$, where, L_2 represents the proportion of total

https://doi.org/10.5194/essd-2026-218
Preprint. Discussion started: 22 April 2026

lime utilized in the chemical industry, and b denotes the share of lime allocated to PCC or SUG production within this sector.

For LM, $M_{lm} = m_{papre} \times r_{lm} \times (1 - U_{lm})$, where m_{papre} is production of paper and paperboard, r_{lm} is the lime mud generation rate, and U_{lm} is the recycling rate. Given the similar physicochemical properties between lime mud and red mud, the carbonation rate of red mud was used as a reference. Consequently, the pile model (Equation 6) was adopted to calculate the carbonation ratio.

For CS, $M_{cs} = m_{lime} \times L_2 \times b_3 \times p_{lime}^{cs} \times r_{cs} \times (1 - U_{cs})$, where, L_2 is the proportion of lime utilized in the chemical industry; b_3 denotes the share of chemical lime allocated to calcium carbide production; p_{lime}^{cs} represents the yield of calcium carbide per ton of lime; r_{cs} is the generation rate of carbide slag; and U_{cs} signifies the utilization rate of the slag.

2.4 Uncertainty Assessment

We identified 18 groups of influencing factors associated with the estimation of carbon emissions and carbon uptake in the lime production process. These factors comprise 1,894 specific input parameters, each characterized by a distinct statistical distribution (see Supplementary Table SI-3 Data1-15). Given the difficulty in obtaining the various values for these parameters, Monte Carlo method recommended by the 2006 IPCC Guidelines for National Greenhouse Gas Inventories was employed to assess the uncertainty associated with the carbon emissions and uptake of lime materials. The statistical characteristics of these 1,894 variables were put into the model and Monte Carlo simulations with 10,000 iterations were performed to generate simulated results for carbon emissions and uptake. Subsequently, statistical analysis was conducted to determine the median values. The 90% confidence intervals (CIs) were calculated using the percentile method; specifically, the 5th and 95th percentiles of the modeled results served as the lower and upper limits of the 90% interval.

Compared with our previous research, this study incorporates refinements in four key aspects. (1) Regional refinement to enhance reference value. We have separated the United Kingdom, France, Germany, Italy, Russia, Japan, Brazil, Australia, and Canada from the ROW category used in previous studies. This allowed to establish a lime carbonation sink dataset for 11 countries for the first time, covering an average of 81.09% of global lime production. (2) More detailed, country-specific parameterization. The parameters were updated for lime CO_2 uptake in the newly added countries. The parameters include the proportion of lime usage across various sectors, the CaO content of different lime materials, and the production and utilization rates of lime materials. These improve the accuracy of the accounting compared to the CO_2 uptake parameters used for the ROW region in our previous work. (3) Inclusion of BFS in the accounting system. the research gap in metallurgical slag carbonation sinks was filled by incorporating BFS. (4) The SS and BFS parameters were updated based on technological evolution across four distinct periods (1930–1950, 1950–1970, 1970–2000, and 2000–2024). By updating the production and utilization rates of steel slag and BFS, the impact of technological progress on carbon sequestration by metallurgical slags were reflected, thereby enhancing the accuracy of historical data.

3. Results and Discussion

3.1 Global Process CO2 Emissions from Lime Production

Figure 2 shows the global process carbon emissions from lime production. Between 1930

https://doi.org/10.5194/essd-2026-218
Preprint. Discussion started: 22 April 2026

Open Access Earth System Science Data Discussions

and 2024, global process CO_2 emissions from the lime industry exhibited a significant upward trend. Annual emissions rose from 113.35Mt CO_2 yr^{-1} (95% CI: 46.43–180.72 Mt CO_2) in 1930 to 299.28 Mt CO_2 yr^{-1} (95% CI: 288.74–310.02 Mt CO_2) in 2024. The cumulative emissions over this period were 15.29 Gt CO_2 (95% CI: 13.81–16.79 Gt CO_2, Fig. 2a). It is driven by the continuous expansion of global urbanization and industrialization. Particularly, the demand for lime in sectors such as construction, metallurgy, chemical engineering, and environmental protection (Wu et al., 2024), increased by approximately 200.8%, growing from 139.62 Mt in 1930 to 420 Mt in 2024 (Lime Statistics and Information | U.S. Geological Survey, 2026) (Supplementary Table SI-2 Data 1).

Statistical analysis reveals a strong correlation between lime carbon emissions and lime production. However, the growth rate of process emissions was lower than that of lime production, suggesting that technological advancements have reduced the carbon emissions intensity of lime production (Laveglia et al., 2024b). From 1930 to 2024, the construction sector accounted for the highest lime-related carbon emissions (Fig. 2b). Emissions increased from 46.61 Mt CO_2 yr^{-1} (95% CI: 11.63–86.62 Mt CO_2) in 1930 to 128.98 Mt CO_2 yr^{-1} (95% CI: 96.26–161.46 Mt CO_2) in 2024. Cumulative emissions from the construction sector reached 5.8 Gt CO_2 (95% CI: 4.11–7.62 Gt CO_2), representing 37.92% of the total cumulative emissions (Fig. 2b). The metallurgical industry followed closely with emissions rising from 36.69 Mt CO_2 yr^{-1} (95% CI: 15.64–64.87 Mt CO_2) in 1930 to 96.51 Mt CO_2 yr^{-1} (95% CI: 66.24–128.95 Mt CO_2) in 2024. This sector contributed 5.04 Gt CO_2 (95% CI: 3.64–6.64 Gt CO_2) cumulatively, accounting for 32.95% of the total (Fig. 2b). Carbon emissions from chemical industry were increasing from 17.70 Mt CO_2 yr^{-1} (95% CI: 8.04–29.16 Mt CO_2) in 1930 to 45.91 Mt CO_2 yr^{-1} (95% CI: 34.64–58.41 Mt CO_2) in 2024. The cumulative emissions for this sector were 2.52 Gt CO_2 (95% CI: 1.91–3.21 Gt CO_2), comprising 16.50% of the total (Fig. 2b). Cumulative carbon emissions from other sectors amounted to 1.93 Gt CO_2 (95% CI: 1.32–2.65 Gt CO_2), accounting for 12.63% of the total.

Between 1930 and 2024, distinct trend in process CO_2 emissions from lime production was observed across different countries. As shown in Fig. 2a, developed nations such as the USA, Germany, France, the UK, and Japan reached their carbon emissions peak around the 1970s, followed by a gradual decline. Notably, emissions in the USA resumed an upward trend entering the 21st century. In contrast, developing countries such as China, Brazil, and Russia generally exhibited an increasing trend in emissions. Specifically, Russia experienced a significant reduction in the 1990s due to the dissolution of the Soviet Union. China emerged as the primary contributor to both global lime production and associated carbon emissions. China's annual emissions rose from 74.34 Mt CO_2 yr^{-1} (95% CI: 7.27–141.63 Mt CO_2) in 1930 to 219.65 Mt CO_2 yr^{-1} (95% CI: 209.36–230.22 Mt CO_2) in 2024, reflecting an average annual growth rate of 1.16%. Cumulative emissions from China were 8.89 Gt CO_2 (95% CI: 7.42–10.36 Gt CO_2), accounting for 58.13% of the global total (Fig. 2b). The USA ranked as the largest emitter among developed nations, with cumulative emissions of 954.03 Mt CO_2 (95% CI: 910.64–997.41 Mt CO_2), representing 6.24% of the global total. Russia (611.06 Mt CO_2), Germany (581.75 Mt CO_2), Japan (408.58 Mt CO_2), Italy (305.00 Mt CO_2), Brazil (258.20 Mt CO_2), and France (189.22 Mt CO_2) contributed 3.99%, 3.8%, 2.67%, 1.99%, 1.68%, and 1.23% to the global total, respectively. The contributions of the United Kingdom (129.43 Mt CO_2),

https://doi.org/10.5194/essd-2026-218
Preprint. Discussion started: 22 April 2026

Australia (76.38 Mt CO_2), and Canada (115.21 Mt CO_2) were relatively small, each accounting for less than 1% (Fig. 2b). Cumulative emissions from the ROW amounted to 2.78 Gt CO_2 (95% CI: 2.65–2.91 Gt CO_2), constituting 18.15% of the global total (Fig. 2b).

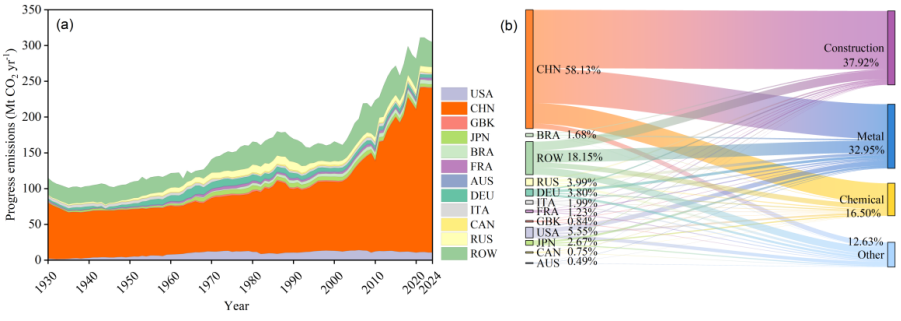

Fig. 2 Global process carbon emissions from lime production. (a) Global annual CO_2 emissions; (b) Cumulative process CO_2 emissions from the lime industry by country and sector.

3.2 Global Carbon Uptake by Lime Carbonation

Global lime carbonation sink increased from 39.34 Mt CO_2 yr^{-1} (95% CI: 12.41–69.76) in 1930 to 167.80 Mt CO_2 yr^{-1} (95% CI: 132.82–209.11) in 2024 (CAGR: 1.55%), with totally accumulative 7.33 Gt CO_2 sink (95% CI: 5.95–8.88) (Fig. 3a). Concurrently, net emissions rose from 74.83 Mt CO_2 yr^{-1} in 1930 to 133.04 Mt CO_2 yr^{-1} in 2024, resulting in cumulative net emissions of 8.00 Gt CO_2 (Fig. 3a). This indicates that lime materials reabsorbed approximately 47.65% of their process emissions (Fig. 3b), about 8.32% increase over previous estimates. The 11 nations contributed 6.03 Gt CO_2 (82.27% of the global total). By refining additional 9 countries' data, the grouped ROW share decreased significantly from 34.35% (Bing et al., 2023) to 17.6% (Fig. 3a). The accounting boundary was improved by including BFS and applying phased parameterization for SS and BFS to reflect technological evolution.

The rising carbon offset level (Fig. 3b) is attributed to the carbonation time lag (Niu et al., 2024). Materials such as MOR, RM, SS, BFS, and LM carbonate over years rather than instantaneously, leading to the accumulative sequestration of historical lime materials legacy. The uncertainty of the updated lime carbonation sink is reduced by 16.58%. The lime carbonation sink in 2024 is equivalent to 1.5%–2% of the 2023 global terrestrial sink (Friedlingstein et al., 2025). This natural and stable "anthropogenic sink" supports IPCC AR6 accounting, enhances GCB completeness, and facilitates global carbon neutrality.

LSS exhibited the highest carbon uptake, with a cumulative absorption of 2.66 Gt CO_2 (95% CI: 1.81–3.67), accounting for 36.53% of the total (Fig. 3d). Its annual uptake reached 59.20 Mt CO_2 yr^{-1} (95% CI: 41.89–78.94) in 2024. MOR followed in second place, contributing a cumulative carbon sink of 1.36 Gt CO_2 (18.66%) (Fig. 3d). SS and BFS ranked third and fourth, respectively: SS accumulated 1.29 Gt CO_2 (17.73%), while BFS—notably a material newly incorporated into this study—achieved a substantial cumulative uptake of 934.83 Mt CO_2 (95% CI: 678.30–1247.10), accounting for 12.83%. Collectively, these four materials contributed 87.47% (7.25 Gt CO_2) of the global lime carbonation sink. In contrast, other materials such as CS, LKD, and PCC made smaller contributions due to their limited production volumes.

https://doi.org/10.5194/essd-2026-218
Preprint. Discussion started: 22 April 2026

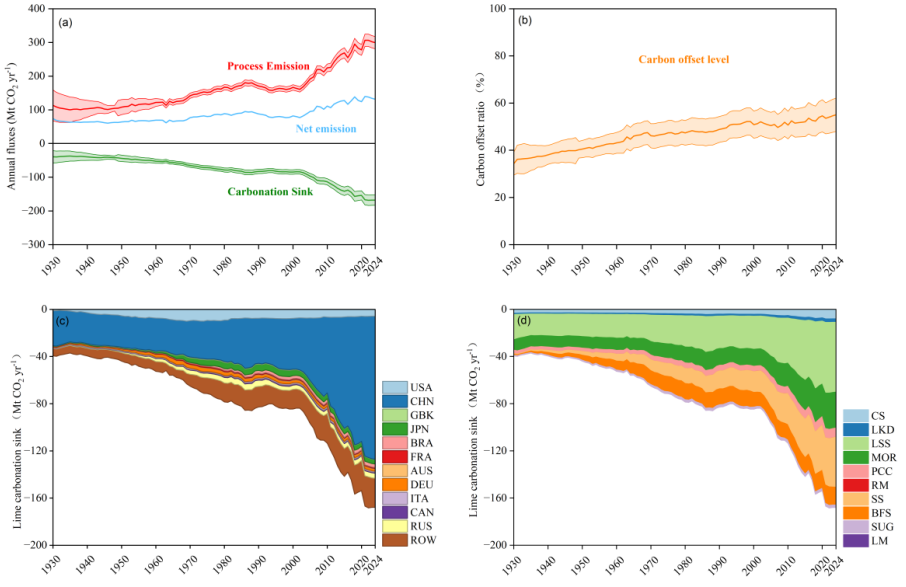

Fig3. (a) Global annual lime process CO_2 emission and carbonation sink;(b) Carbon offset level (ratio of carbonation sink to process CO_2 emission); (c) Annual carbonation sink of lime materials by country and region; (d) Annual carbonation sink of different lime materials

China's lime carbonation sink was increasing from 29.6 Mt CO_2 yr^{-1} (95% CI: 2.82–59.84) in 1930 to 121.27 Mt CO_2 yr^{-1} (95% CI: 88.13–160.49) in 2024. Cumulative uptake reached 4.21 Gt CO_2 (95% CI: 2.75–6.01 Gt), accounting for 57.45% of the global total (Fig. 3c), which is driven by sustained demand from large-scale construction and iron & steel industries. The United States is the largest contributor among developed nations, with annual lime carbonation sink rising from 1.22 Mt CO_2 yr^{-1} (95% CI: 0.83–1.74) to 5.79 Mt CO_2 yr^{-1} (95% CI: 4.29–7.53). Its cumulative uptake of 625.16 Mt CO_2 (95% CI: 451.77–839.45) represents 8.52% of the global total. The contributions from Russia (285.67 Mt CO_2), Germany (193.82 Mt CO_2), Japan (296.69 Mt CO_2), Brazil (132.20 Mt CO_2), and Italy (87.97 Mt CO_2) accounted for 3.89%, 2.64%, 4.05%, 1.80%, and 1.19%, respectively (Fig. 3c). In contrast, France, the United Kingdom, Australia, and Canada each contributed less than 1%, directly reflecting their limited lime production.

3.3 Global Lime Carbonation Sink in Different Industries

Industry-based analysis indicates that global carbon uptake by lime-based materials exhibited a persistent increasing trend across all major industrial sectors from 1930 to 2024. However, substantial inter-sectoral differences are observed in terms of carbonation sink magnitude, dominant material types, and evolutionary pathways (Fig. 4). Overall, the construction sector represents the core contributor to the global lime carbonation sink, followed by the metallurgical sector, while the chemical industry provides a small yet stable contribution.

Carbon uptake in the construction sector increased from 30.14 Mt CO_2 yr^{-1} in 1930 (95% CI: 7.42–59.34) to 89.63 Mt CO_2 yr^{-1} in 2024 (95% CI: 55.72–133.23, Fig. 3a). The cumulative carbonation sink over the study period reached 4.02 Gt CO_2 (95% CI: 2.59–5.79), accounting

https://doi.org/10.5194/essd-2026-218
Preprint. Discussion started: 22 April 2026

for 57.45% of the global lime carbonation sink (Fig. 4). This dominant contribution is primarily attributable to the high penetration of lime-based materials in the construction sector and the sustained mineral carbonation occurring throughout their long service life. As a key pillar of global infrastructure development and urban expansion, the construction sector has maintained the largest share of lime-related carbon sequestration throughout the entire study period due to its substantial demand for lime materials. In particular, since the latter half of the twentieth century, accelerated global urbanization and infrastructure investment have markedly expanded the use of lime-based materials, thereby driving a rapid increase in carbon uptake within this sector (Manzoor and Yousuf, 2020). The synergistic effects among different lime materials within the construction sector have continuously amplified its overall carbonation sink capacity at the global scale, underscoring its central role in the lime-based carbon sequestration.

The metallurgical sector constitutes the second-largest global lime carbonation sink, with a cumulative carbon uptake of 2.23 Gt CO_2 (95% CI: 1.76–2.77), accounting for 30.56% of the total carbonation sink. Lime-based materials generated during metallurgical processes, particularly in iron and steel production, provide a substantial material basis for mineral carbonation. With the sustained growth of global iron and steel output over the past century, the carbon sequestration potential of slags in the metallurgical sector has increased significantly. Notably, by incorporating refined historical-stage parameters, this study systematically accounts for variations in the generation rates and utilization efficiencies of metallurgical by-products across countries, thereby substantially improving the reliability of carbonation sink estimates for this sector. Previous studies have demonstrated pronounced cross-country differences in slag and blast furnace residue management strategies (Guo et al., 2018; USGS, 2026b; O'Connor et al., 2021; Horii et al., 2015), which showed developed countries established relatively mature resource utilization systems at an early stage, whereas developing countries have gradually transitioned from long-term stockpiling toward more efficient and comprehensive utilization ways. The combined effects of technological advancement and policy intervention have played a decisive role in shaping the long-term accumulation of the metallurgical lime carbonation sink.

The chemical industry contributes a relatively smaller share to the global lime carbonation sink, with a cumulative carbon uptake of 1.79 Gt CO_2 (95% CI: 1.05–2.78), accounting for 12.22% of the global total. In the chemical sector, lime-based materials sequester CO_2 mainly through industrial carbonation reactions, and their contribution has increased steadily over the study period, providing an important component to the global lime carbonation sink.

From spatial perspective, industry-dominated patterns of lime carbon sequestration exhibit pronounced heterogeneity across countries and regions (Fig. 4). Developed countries (e.g., the United States, Japan, and major European nations), characterized by long histories of iron and steel production and well-established circular economy systems, have long been dominated by metallurgical-sector lime carbonation sink, with cumulative effects that are particularly evident on historical timescales (Spring and Cirella, 2022). In contrast, developing countries undergoing rapid industrialization and urbanization (e.g., China, Brazil, and parts of the rest-of-world regions) have experienced surging demand for lime-based materials in the construction sector, which has gradually become the primary regional source of lime-related carbon sequestration. In China, carbon uptake by lime materials in the construction sector

https://doi.org/10.5194/essd-2026-218
Preprint. Discussion started: 22 April 2026

accelerated markedly in the early twenty-first century, closely coinciding with the timing of rapid urbanization (Cai et al., 2020).

Overall, the differentiated global distribution of lime carbonation sink across industries and regions fundamentally reflects the combined influences of industrial structure, economic development pathways, resource utilization efficiency, and policy frameworks. Clarifying the relative contributions of different sectors and their underlying evolutionary mechanisms is of critical scientific importance for designing sector-specific carbon management strategies for enhancing the carbon sequestration potential of lime-based materials.

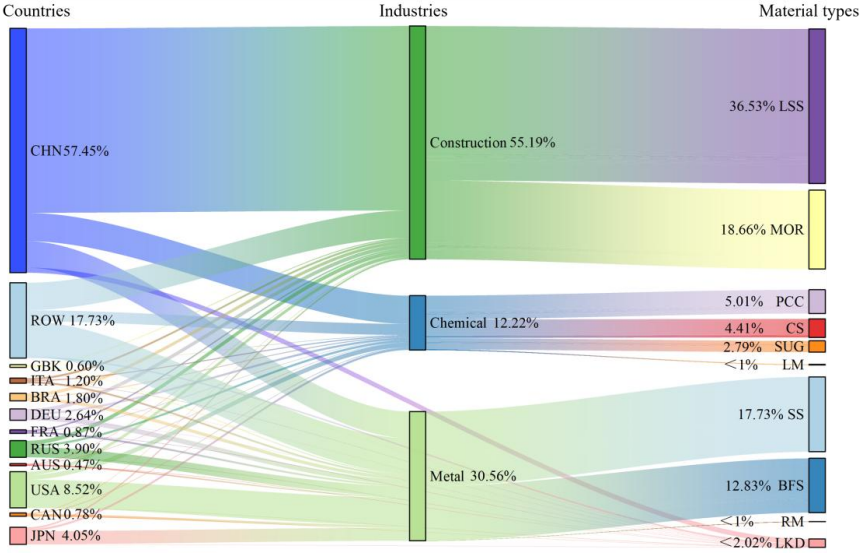

Fig 4. Global Cumulative Lime Carbonation Sink in different countries, industries, and material types, 1930–2024

3.4 Time-Lag Effect of Lime Carbonation Sink

Based on estimates, both current-year and historical CO_2 uptake by global lime materials exhibited continuous growth trends (Fig. 5a). "Current-year uptake" refers to CO_2 absorbed by materials produced within the same year, whereas "historical uptake" denotes CO_2 sequestered in subsequent years by previously produced but uncarbonated materials.

Current-year uptake rose from 38.52 Mt CO_2 yr^{-1} in 1930 to 118.65 Mt CO_2 yr^{-1} in 2024 (CAGR: 0.96%), with a cumulative total of 5.48 Gt CO_2, representing 75.24% of the total uptake. Conversely, historical uptake increased significantly from 1.99 Mt CO_2 yr^{-1} in 1931 to 47.59 Mt CO_2 yr^{-1} in 2024 (CAGR: 2.12%), accumulating 1.77 Gt CO_2 (24.35% of the total) (Fig. 5a). LSS is the primary contributor to current-year uptake, accumulating 2.62 Gt CO_2 (35.94% of the current cumulative total), followed by MOR with 1.04 Gt CO_2 (14.23%). In contrast, SS dominates historical uptake, accumulating 949.65 Mt CO_2 (53.78% of the historical cumulative total), followed by BFS with 570.33 Mt CO_2 (32.23%) (Supplementary Table SI-1 Data 6). These results highlight the distinct temporal mechanisms of carbon uptake across different lime materials (Fig. 5b). Historical uptake for SS and BFS exceeds their current-year uptake because their carbonation is not instantaneous (Liu et al., 2018), and the majority occurs

https://doi.org/10.5194/essd-2026-218
Preprint. Discussion started: 22 April 2026

in subsequent years. Additionally, environmental conditions such as temperature and humidity influence the natural carbonation rates of SS and BFS (Zhao et al., 2025). Future efforts should leverage Carbon Capture, Utilization, and Storage (CCUS) technologies to achieve efficient sequestration (Yang et al., 2022).

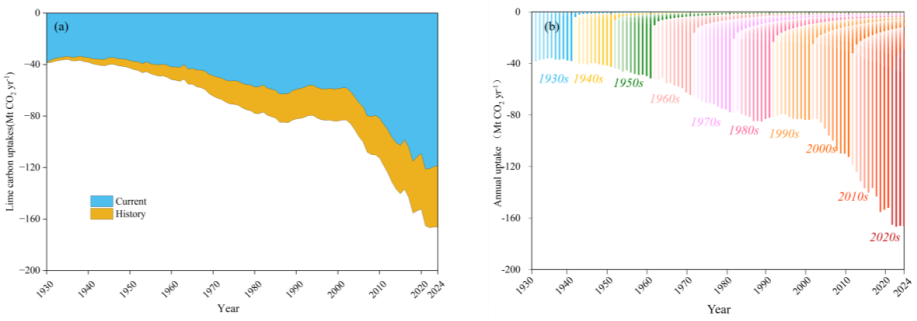

Fig5. Delayed Effects of Lime Carbon Absorption, 1930–2024. (a) global lime annual CO2 uptake in current and historical year; (b) global annual uptake of atmospheric CO2 by lime, disaggregated by years of production.

3.5 Peaking Trajectories and Regional Disparities in Lime Carbon Balance

Based on lime process emissions and carbonation sink data, this study reveals significant regional heterogeneity in global lime carbon balance: developed nations (e.g., in Europe and North America) have achieved carbon peaking, whereas most developing countries (e.g., China and Brazil) remain in a growth trend.

In developed countries, CO_2 emissions peaked between the 1960s and early 2000s. Germany (1964, 12.73 Mt CO_2), France (1974, 3.72 Mt CO_2), Japan (1979, 7.01 Mt CO_2), and the UK (1980, 2.90 Mt CO_2) peaked earlier, followed by Canada (1999, 1.89 Mt CO_2), the USA (2006, 15.57 Mt CO_2), Italy (2008, 4.39 Mt CO_2), and Australia (2011, 1.81 Mt CO_2). The carbon offset levels at their peaks were: 74.09% (Japan), 50.05% (Canada), 47.54% (USA), 33.55% (Australia), 28.15% (UK), 29.67% (France), and 25.00% (Germany), respectively. Following the peak year, carbon emissions from lime production in these nations have exhibited downward trend, with annual decline rates ranging from 0.8% to 5.2%. Carbonation sink has also gradually decreased with lime production reduction. However, due to the time-lag effect inherent in the carbonation of certain lime-based materials, the decline in carbon uptake has been less pronounced than that of emissions. Consequently, the carbon offset level has progressively increased, suggesting that future net emissions may approach zero or even achieve negative values, thereby facilitating the realization of carbon neutrality within the lime production sector. This characteristic is fundamentally attributed to the establishment of mature secondary resource recycling systems and stringent climate policy constraints in developed nations (Dolphin et al., 2023), particularly the high recovery and comprehensive utilization of metallurgical by-products such as BFS and SS (Yi et al., 2012). In the fields of construction and civil engineering, the substitution of primary lime materials with these alkaline solid wastes not only substantially mitigates process-related carbon emissions during production but also effectively sustains the carbonation sink potential through continuous mineral carbonation

https://doi.org/10.5194/essd-2026-218
Preprint. Discussion started: 22 April 2026

during the full life cycle of their secondary application (Pan et al., 2017).

Conversely, developing countries exhibit continuous process emissions growth. China's lime process emissions have risen since 1930 (CAGR: 1.16%), accelerating to 3.69% annually post-2002 due to urbanization and infrastructure demands. Lime process emissions in China reached 219.64 Mt CO_2 yr^{-1} in 2024. Despite a high offset level of 55.21% (121.27 Mt CO_2 yr^{-1}), abatement pressure remains high. Lime process emissions in Brazil reached 5.89 Mt CO_2 yr^{-1} in 2024 (offset: 50.11%). Although Russia peaked during the Soviet era, emissions rebounded after 2000 (CAGR: 1.34%), reaching 8.04 Mt CO_2 yr^{-1} in 2024 (offset: 53.87%). Lime process emissions growth in these regions is driven by infrastructure demands amidst industrialization and urbanization (Chen et al., 2022), while Russia's rebound correlates with economic recovery and industrial capacity restoration post-2000.

In summary, the regional differentiation in process emissions and carbonation sink trajectories reflect distinct development stages. Developed countries achieved inflection points through industrial transformation and policy intervention, whereas developing countries face the dual challenge of economic growth and carbon emissions reduction. Furthermore, the divergence in carbon offset levels further reflects the disparities in the resource recycling efficiency of lime materials across nations.

https://doi.org/10.5194/essd-2026-218
Preprint. Discussion started: 22 April 2026

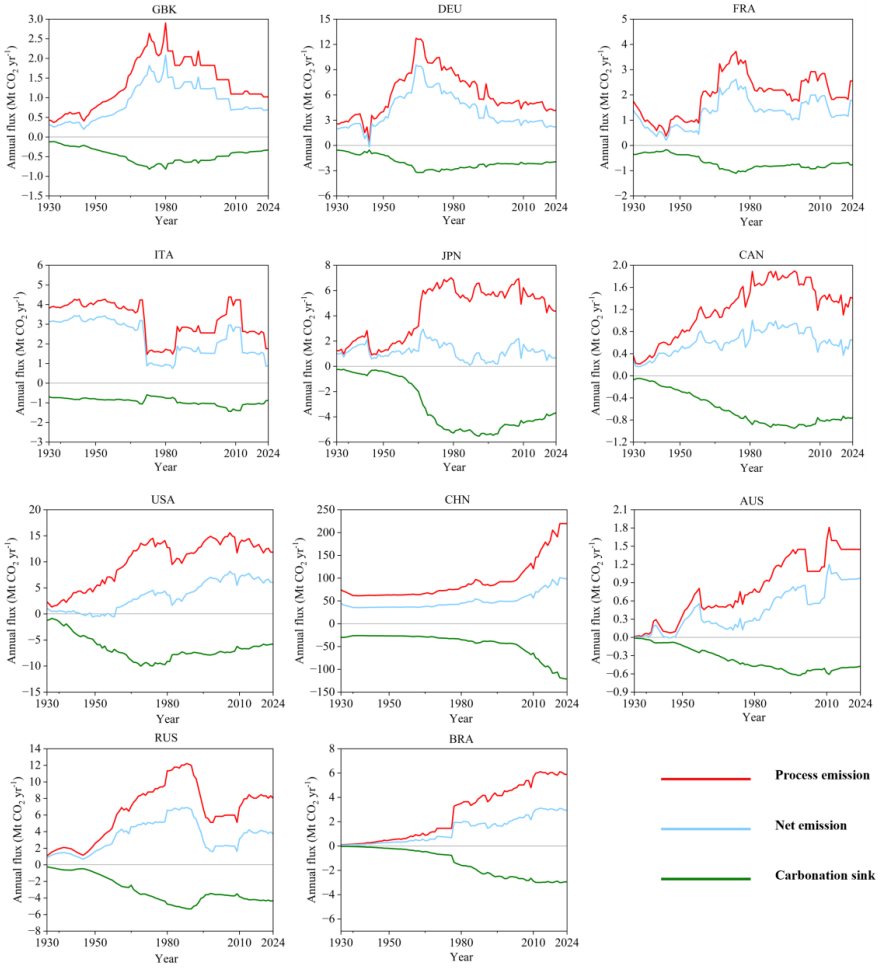

Fig 6. Lime process emissions, carbonation sink, and net emissions in 11 Countries from 1930 to 2024

3.6 Uncertainty Analysis

Based on the accounting model established by (Xi et al., 2016) and the research framework of (Bing et al., 2023), this study incorporates new data on lime process emissions and carbonation sink for nine additional countries. Particular emphasis was placed on the CaO content of lime in different application industries, which is identified as the most significant factor influencing carbonation sink (Niu et al., 2024). Following IPCC recommendations, a Monte Carlo analysis with 10,000 iterations was conducted to quantify the uncertainties lime process emissions and carbonation sink. (Detailed uncertainty coefficients for lime material carbon sequestration by country are presented in Supplementary Table SI-3 Data1-15.)

The results indicate that the global cumulative process emissions in this study amount to 15.29 Gt CO_2 (95% CI: 13.81–16.79 Gt CO_2), while the global cumulative lime carbonation sink is 7.33 Gt CO_2 (95% CI: 5.95–8.88 Gt CO_2). Compared to the previous estimates by Bing

https://doi.org/10.5194/essd-2026-218
Preprint. Discussion started: 22 April 2026

et al. (2023) that reported 13.64 Gt CO_2 (95% CI: 11.61–15.72 Gt CO_2) and 5.29 Gt CO_2 (95% CI: 3.73–7.19 Gt CO_2), they increase 12.1% and 38.43%, respectively. The annual lime carbonation sink in 2020 reached 153.67 Mt CO_2 (95% CI: 122.63–190.35 Mt CO_2), which showed 20.31% increase over the 127.73 Mt CO_2 (95% CI: 86.17–182.72 Mt CO_2) reported in the previous study. Consequently, the cumulative carbon offset level (carbonation sink divide process emissions) rose from 38.83% to 47.65%, with an increase of 8.32%. Furthermore, the contribution of metallurgical slags to total lime carbonation sink increased from 15.62% to 26.9%, reflecting a growth of 11.23% impacted by BSF inclusion. Meanwhile, China's share of cumulative carbonation sink was adjusted from 63.95% to 57.45%.

These discrepancies stem from quantifiable methodological optimizations rather than data contradictions. The increase of global lime carbonation sink is jointly driven by the temporal extension, the expansion of accounting boundary, and country-specific data refinement. The inclusion of data for four additional years (2021–2024) based on USGS global lime production statistics (reaching 420 million tonnes in 2024, with China accounting for 73.81%) contributed an additional 746.79 Mt CO_2 in carbon sequestration, accounting for 9.01% of the total. Moreover, the incorporation of BFS into the accounting boundary combined with solid waste statistics from China's steel industry, where BFS constitutes over 50% of total iron and steel solid waste (Pan et al., 2017), quantified a contribution of 934.83 Mt CO_2. This accounts for 11.27% of the total, effectively filling a critical gap in the carbonation sink accounting for metallurgical slags. Additionally, by refining 11 core parameters on a country-specific data (e.g., correcting China's steel slag generation rate to 0.12–0.15 t/t crude steel for specific time periods), the width of the 95% CI in this study was reduced by 12.47% compared to Bing et al. (Bing et al., 2023), indicating a significant reduction in uncertainty.

4. Data Availability

The datasets generated and analyzed in this study are available in the Zenodo repository: https://doi.org/10.5281/zenodo.18616060 (Bing et al., 2026). The dataset comprises three data files, including the results of lime-related carbon emissions and CO_2 uptake (Supplementary Table SI-1), basic activity data for lime-based materials (Supplementary Table SI-2), and uncertainty parameters associated with lime carbon emissions and CO_2 uptake (Supplementary Table SI-3).

5. Conclusion

In this study, we further advanced the high-resolution accounting of global carbon emissions and uptake within the lime industry. For emission accounting, we extended the temporal scope to the period of 1930–2024 and refined the spatial resolution to 11 major producing countries, capturing 87.62% of total global production. Furthermore, accounting uncertainties were significantly mitigated by deriving localized emission factors based on the specific calcium oxide requirements and consumption structures of downstream industries. Our results demonstrate that cumulative emissions reached 15.33 Gt CO_2 (95% CI: 13.15–17.58 Gt CO_2) between 1930 and 2024. The construction sector emerged as the primary emission source, cumulatively releasing 5.8 Gt CO_2, followed by the metallurgical (5.04 Gt CO_2) and chemical (2.55 Gt CO_2) sectors.

Regarding carbon uptake, we expanded the system boundary by incorporating blast furnace slag (BFS) into the accounting framework for the first time, and dynamically updated

https://doi.org/10.5194/essd-2026-218
Preprint. Discussion started: 22 April 2026

the output and utilization parameters of steel slag (SS) and BFS in distinct phases to reflect the technological evolution of the iron and steel industry. During the same period, global lime materials cumulatively sequestered 7.33 Gt CO_2 (95% CI: 5.66–9.32 Gt CO_2). This carbonation sink offsets approximately 47.65% of historical process emissions and represents roughly 1.5%–2% of the 2023 global terrestrial carbon sink. China remains the dominant contributor, with a cumulative uptake of 4.21 Gt CO_2 (95% CI: 2.75–6.01 Gt CO_2), representing 57.45% of the global total. LSS, MOR, SS, and BFS were identified as the primary sequestering materials, contributing 36.53%, 18.66%, 17.73%, and 12.83% to the total sink, respectively (collectively 85.75%). Historically, SS and BFS played the most significant roles in sequestration, accounting for 53.78% and 32.23% of the cumulative historical uptake.

Regional divergence of lime carbonation sink is pronounced. Carbon sequestration is primarily from LSS, MOR, and SS in developing nations such as China and Brazil, whereas dominant from SS and BFS in developed regions like the United States. Developed economies, including Europe, the United States Japan, and Australia, have already achieved carbon peaks, characterized by declining gross emissions and net emissions approaching zero. In contrast, developing nations continue to show simultaneous growth in both emissions and uptake. Despite maintaining high offset levels, these regions face acute pressure from rising absolute emission volumes. These findings underscore the critical carbon sink value of the lime industry and provide a new lens through which to view global carbon neutrality pathways. Furthermore, the enhanced accounting precision provided by this study offers the necessary empirical support for incorporating lime carbon uptake into the Global Carbon Budget.

Author Contributions. F.X. designed and supervised the project. X.Z., with assistance from L.N., carried out data collection, organization, data analysis, and database construction. L.B. was responsible for developing and parameterizing the accounting model, writing the computational code, and generating the integrated accounting results. The manuscript was primarily drafted by X.Z. and L.B., and further improved through important suggestions and contributions from J.W., J.L., J.X., and F.X.

Competing interests. The contact author has declared that none of the authors has any competing interests.

Acknowledgements. We thank our colleagues at the Institute of Applied Ecology, Chinese Academy of Sciences for their insightful discussions and technical support during the data collection and analysis phases. We also appreciate the constructive comments from the editors and anonymous reviewers of Earth System Science Data, which significantly improved the quality of this manuscript.

Financial support. This research was supported by Joint Foundation Project of Liaoning Province, 2023-MSBA-141, the Major Program of the Institute for Applied Ecology of the Chinese Academy of Sciences (No. IAEMP202201), Technology Innovation and Management of the Whole Process Green Development of Mineral Resources (No. 2023-JB-09-07), and Key Research and Development Project of Liaoning Province (No. 2025JH2/101330021).

https://doi.org/10.5194/essd-2026-218
Preprint. Discussion started: 22 April 2026

Reference

Andrew, R. M.: Global CO_2 emissions from cement production, 1928–2018, Earth Syst. Sci. Data, 11, 1675–1710, https://doi.org/10.5194/essd-11-1675-2019 , 2019.

Annuaire Statistique de la France archives(ASF): https://onlinebooks.library.upenn.edu/webbin/serial?id=annstatfr , (last access: 18 January 2026), 2026.

Australian Bureau of Statistics(ABS): https://www.abs.gov.au/ , (last access: 18 January 2026), 2026.

Brazilian Institute of Geography and Statistics (IBGE): https://www.abc.gov.br/training/informacoes/InstituicaoIBGE_en.aspx (last access: 18 January 2026), 2026.

British Geological Survey (BGS): https://www.bgs.ac.uk/mineralsuk/statistics/world-mineral-statistics/world-mineral-statistics-archive/ (last access: 18 January 2026), 2026.

Bing, L., Zhang, X., Wang, J., Niu, L., and Xi, F.: Global and National CO2 Emission from Lime Production Process and Carbonation sink from 1930 to 2024 (2.0), Zenodo [Data set], https://doi.org/10.5281/zenodo.18616060, 2026.

Bing, L., Ma, M., Liu, L., Wang, J., Niu, L., and Xi, F.: An investigation of the global uptake of CO_2 by lime from 1930 to 2020, Earth Syst. Sci. Data, 15, 2431–2444, https://doi.org/10.5194/essd-15-2431-2023 , 2023.

Cai, Z., Liu, Q., and Cao, S.: Real estate supports rapid development of China's urbanization, Land Use Policy, 95, 104582, https://doi.org/10.1016/j.landusepol.2020.104582, 2020.

Campo, F. P., Tua, C., Biganzoli, L., Pantini, S., and Grosso, M.: Natural and enhanced carbonation of lime in its different applications: a review, Environ. Technol. Rev., https://doi.org/10.1080/21622515.2021.1982023 , 2021.

China Building Materials Enterprise Management Association (CBMEMA): Carbon Emission Report of China's Building Materials Industry, https://www.bmema.org/xiehuidongtai/161.html (last access: 18 January 2026), 2026.

Chen, C., Xu, R., Tong, D., Qin, X., Cheng, J., Liu, J., Zheng, B., Yan, L., and Zhang, Q.: A striking growth of CO2 emissions from the global cement industry driven by new facilities in emerging countries, Environ. Res. Lett., 17, 044007, https://doi.org/10.1088/1748-9326/ac48b5, 2022.

https://doi.org/10.5194/essd-2026-218
Preprint. Discussion started: 22 April 2026

748 Davis, S. J., Lewis, N. S., Shaner, M., Aggarwal, S., Arent, D., Azevedo, I. L., Benson, S. M.,
749 Bradley, T., Brouwer, J., Chiang, Y.-M., Clack, C. T. M., Cohen, A., Doig, S., Edmonds, J.,
750 Fennell, P., Field, C. B., Hannegan, B., Hodge, B.-M., Hoffert, M. I., Ingersoll, E., Jaramillo,
751 P., Lackner, K. S., Mach, K. J., Mastrandrea, M., Ogden, J., Peterson, P. F., Sanchez, D. L.,
752 Sperling, D., Stagner, J., Trancik, J. E., Yang, C.-J., and Caldeira, K.: Net-zero emissions energy
753 systems, Science, 360, eaas9793, https://doi.org/10.1126/science.aas9793 , 2018.

754 Dolphin, G., Pahle, M., Burtraw, D., and Kosch, M.: A net-zero target compels a backward
755 induction approach to climate policy, Nat. Clim. Change, 13, 1033–1041,
756 https://doi.org/10.1038/s41558-023-01798-y , 2023.

757 Dominion Bureau of Statistics, Mining, Metallurgical and Chemical Branch: Statistics
758 publication, Dominion Bureau of Statistics, Ottawa, Canada, available at:
759 https://publications.gc.ca/site/eng/9.847247/publication.html . last access: 18 January 2026.

760 Ellis, L. D., Badel, A. F., Chiang, M. L., Park, R. J.-Y., and Chiang, Y.-M.: Toward
761 electrochemical synthesis of cement—An electrolyzer-based process for decarbonating $CaCO_3$
762 while producing useful gas streams, Proc. Natl. Acad. Sci., 117, 12584–12591,
763 https://doi.org/10.1073/pnas.1821673116 , 2020.

764 European Lime Association (EuLA): A PATHWAY TO NEGATIVE CO2 EMISSIONS BY
765 2050,https://eula.eu/wp-content/uploads/2023/09/WEB_EULA-2030-Climate-
766 Roadmap_Lime-Acts_A4_v19.pdf (last access: 18 January 2026), 2026a.

767 European Lime Association (EuLA): Lime as a Natural Carbon Sink, https://eula.eu/wp-
768 content/uploads/2023/11/LIME-AS-A-NATURAL-CARBON-SINK.pdf (last access: 18
769 January 2026), 2026b.

770 European Commission. Joint Research Centre. Institute for Prospective Technological Studies.:
771 Best available techniques (BAT) reference document for the production of cement, lime and
772 magnesium oxide: Industrial Emissions Directive 2010/75/EU (integrated pollution prevention
773 and control), Publications Office, LU, 2013.

774 Food and Agriculture Organization of the United Nations (FAO): https://www.fao.org/forestry-
775 fao/statistics/80570/en/ (last access: 18 January 2026), 2026.

776 Friedlingstein, P., O'sullivan, M., Jones, M. W., Andrew, R. M., Hauck, J., Olsen, A., Peters, G.
777 P., Peters, W., Pongratz, J., and Sitch, S.: Global carbon budget 2020, Earth Syst. Sci. Data
778 Discuss., 2020, 1–3, https://doi.org/10.5194/essd-12-3269-2020 ,2020.

779 Friedlingstein, P., O'Sullivan, M., Jones, M. W., Andrew, R. M., Gregor, L., Hauck, J., Le Quéré,
780 C., Luijkx, I. T., Olsen, A., Peters, G. P., Peters, W., Pongratz, J., Schwingshackl, C., Sitch, S.,
781 Canadell, J. G., Ciais, P., Jackson, R. B., Alin, S. R., Alkama, R., Arneth, A., Arora, V. K., Bates,

https://doi.org/10.5194/essd-2026-218
Preprint. Discussion started: 22 April 2026

N. R., Becker, M., Bellouin, N., Bittig, H. C., Bopp, L., Chevallier, F., Chini, L. P., Cronin, M., Evans, W., Falk, S., Feely, R. A., Gasser, T., Gehlen, M., Gkritzalis, T., Gloege, L., Grassi, G., Gruber, N., Gürses, Ö., Harris, I., Hefner, M., Houghton, R. A., Hurtt, G. C., Iida, Y., Ilyina, T., Jain, A. K., Jersild, A., Kadono, K., Kato, E., Kennedy, D., Klein Goldewijk, K., Knauer, J., Korsbakken, J. I., Landschützer, P., Lefèvre, N., Lindsay, K., Liu, J., Liu, Z., Marland, G., Mayot, N., McGrath, M. J., Metzl, N., Monacci, N. M., Munro, D. R., Nakaoka, S.-I., Niwa, Y., O'Brien, K., Ono, T., Palmer, P. I., Pan, N., Pierrot, D., Pocock, K., Poulter, B., Resplandy, L., Robertson, E., Rödenbeck, C., Rodriguez, C., Rosan, T. M., Schwinger, J., Séférian, R., Shutler, J. D., Skjelvan, I., Steinhoff, T., Sun, Q., Sutton, A. J., Sweeney, C., Takao, S., Tanhua, T., Tans, P. P., Tian, X., Tian, H., Tilbrook, B., Tsujino, H., Tubiello, F., van der Werf, G. R., Walker, A. P., Wanninkhof, R., Whitehead, C., Willstrand Wranne, A., et al.: Global Carbon Budget 2022, Earth Syst. Sci. Data, 14, 4811–4900, https://doi.org/10.5194/essd-14-4811-2022 , 2022.

Friedlingstein, P., O'sullivan, M., Jones, M. W., Andrew, R. M., Hauck, J., Landschützer, P., Le Quéré, C., Li, H., Luijkx, I. T., and Olsen, A.: Global carbon budget 2024, Earth Syst. Sci. Data Discuss., 2024, 1–133, https://doi.org/10.5194/essd-17-965-2025, 2025.

Gao, W., Zhou, W., Lyu, X., Liu, X., Su, H., Li, C., and Wang, H.: Comprehensive utilization of steel slag: A review, Powder Technol., 422, 118449, https://doi.org/10.1016/j.powtec.2023.118449, 2023.

Gomari, K. E., Gomari, S. R., Hughes, D., and Ahmed, T.: Exploring the potential of steel slag waste for carbon sequestration through mineral carbonation: A comparative study of blast-furnace slag and ladle slag, J. Environ. Manage., 351, 119835, https://doi.org/10.1016/j.jenvman.2023.119835, 2024.

Guo, J., Bao, Y., and Wang, M.: Steel slag in China: Treatment, recycling, and management, Waste Manag., 78, 318–330, https://doi.org/10.1016/j.wasman.2018.04.045, 2018.

Han, R., Wang, Y., Xing, S., Pang, C., Hao, Y., Song, C., and Liu, Q.: Progress in reducing calcination reaction temperature of Calcium-Looping CO2 capture technology: A critical review, Chem. Eng. J., 450, 137952, https://doi.org/10.1016/j.cej.2022.137952 , 2022.

Hanein, T., Simoni, M., Woo, C. L., Provis, J. L., and Kinoshita, H.: Decarbonisation of calcium carbonate at atmospheric temperatures and pressures, with simultaneous CO 2 capture, through production of sodium carbonate, Energy Environ. Sci., 14, 6595–6604, https://doi.org/10.1039/D1EE02637B, 2021.

Heraiz, H., Li, J., Pan, Z., Zhang, D., Hu, Y., Mu, X., Baras, A., Liu, J., Ni, W., and Hitch, M.: The Utilization of Slag, Steel Slag, and Desulfurization Gypsum as Binder Systems in UHPC with Iron Tailings and Steel Fibers—A Review, Minerals, 15, 538, https://doi.org/10.3390/min15050538, 2025.

https://doi.org/10.5194/essd-2026-218
Preprint. Discussion started: 22 April 2026

817 Horii, K., Tsutsumi, N., Kato, T., Kitano, Y., and Sugahara, K.: Overview of iron/steel slag
818 application and development of new utilization technologies, Nippon Steel Sumitomo Met.
819 Tech. Rep., 109, 5–11, https://www.nipponsteel.com/en/tech/report/nssmc/pdf/109-03.pdf,
820 2015.

821 Huang, Z., Wang, J., Bing, L., Qiu, Y., Guo, R., Yu, Y., Ma, M., Niu, L., Tong, D., and Andrew,
822 R. M.: Global carbon uptake of cement carbonation accounts 1930–2021, Earth Syst. Sci. Data
823 Discuss., 2023, 1–28, https://doi.org/10.5194/essd-15-4947-2023, 2023.

824 IPCC: IPCC guidelines for national greenhouse gas inventories, Institute for Global
825 Environmental Strategies (IGES), Hayama (Japan), 2006.

826 Laveglia, A., Ukrainczyk, N., De Belie, N., and Koenders, E.: Cradle-to-grave environmental
827 and economic sustainability of lime-based plasters manufactured with upcycled materials, J.
828 Clean. Prod., 452, 142088, https://doi.org/10.1016/j.jclepro.2024.142088 , 2024a.

829 Laveglia, A., Ukrainczyk, N., De Belie, N., and Koenders, E.: From quarry to carbon sink:
830 process-based LCA modelling of lime-based construction materials for net-zero and carbon-
831 negative transformation, Green Chem., 26, 6584–6600, https://doi.org/10.1039/D3GC04599D,
832 2024b.

833 Liu, L. L., Wang, J. Y., Bing, L. F., Ling, J. H., Xu, M., and Xi, F. M.: Analysis of carbon sink
834 of steel slag in China., Ying Yong Sheng Tai Xue Bao J. Appl. Ecol., 29, 3385–3390,
835 https://doi.org/10.13287/j.1001-9332.201810.015, 2018.

836 Liu, Z., Guan, D., Wei, W., Davis, S. J., Ciais, P., Bai, J., Peng, S., Zhang, Q., Hubacek, K., and
837 Marland, G.: Reduced carbon emission estimates from fossil fuel combustion and cement
838 production in China, Nature, 524, 335–338, https://doi.org/10.1038/nature14677, 2015.

839 Ministry of Industry and Information Technology(MIIT): Implementation Plan for Achieving
840 the Carbon Peak in the Building Materials
841 Industry,https://www.gov.cn/zhengce/zhengceku/2022-11/08/content_5725353.htm , last
842 access: 18 January 2026.

843 Manocha, S. and Ponchon, F.: Management of lime in steel, Metals, 8, 686,
844 https://doi.org/10.3390/met8090686, 2018.

845 Manzoor, S. O. and Yousuf, A.: Stabilisationof soils with lime: A review, J Mater Env. Sci, 11,
846 1538–1551, 2020.

847 Naito, M., Takeda, K., and Matsui, Y.: Ironmaking technology for the last 100 years:
848 deployment to advanced technologies from introduction of technological know-how, and
849 evolution to next-generation process, ISIJ Int., 55, 7–35,

https://doi.org/10.5194/essd-2026-218
Preprint. Discussion started: 22 April 2026

https://doi.org/10.2355/isijinternational.55.7, 2015.

Niu, L., Wu, S., Andrew, R. M., Shao, Z., Wang, J., and Xi, F.: Global and national CO 2 uptake by cement carbonation from 1928 to 2024, Earth Syst. Sci. Data Discuss., 2024, 1–23, https://doi.org/10.5194/essd-17-2231-2025, 2024.

Nation Lime Association(NLA): A ROADMAP TO CARBON NEUTRALITY FOR THE U.S. LIMEINDUSTRY,https://www.lime.org/wpcontent/uploads/nla_lime_roadmap_final_01_july_24_cc.pdf (last access: 18 January 2026), 2026.

Ordnance Survey, Ten-mile to the Inch, Planning Maps of Great Britain - 1940s-1970s - National Library of Scotland: https://maps.nls.uk/os/ten-mile/info.html (last access: 18 January 2026), 2026.

O'Connor, J., Nguyen, T. B. T., Honeyands, T., Monaghan, B., O'Dea, D., Rinklebe, J., Vinu, A., Hoang, S. A., Singh, G., and Kirkham, M. B.: Production, characterisation, utilisation, and beneficial soil application of steel slag: A review, J. Hazard. Mater., 419, 126478, https://doi.org/10.1016/j.jhazmat.2021.126478Get rights and content, 2021.

Pan, S.-Y., Chung, T.-C., Ho, C.-C., Hou, C.-J., Chen, Y.-H., and Chiang, P.-C.: CO2 mineralization and utilization using steel slag for establishing a waste-to-resource supply chain, Sci. Rep., 7, 17227, https://dx.doi.org/10.1038/s41598-017-17648-9, 2017.

Ren, S., Aldahri, T., Liu, W., and Liang, B.: CO2 mineral sequestration by using blast furnace slag: From batch to continuous experiments, Energy, 214, 118975, https://doi.org/10.1016/j.energy.2020.118975, 2021.

Revuelta, M. B.: Construction Materials: Geology, Production and Applications, Springer Nature, 602 pp. https://doi.org/10.1007/978-3-030-65962-1, 2021.

Shimnishi, T. : A History of Limestone Mining Industry in the Postwar Period, Based on LIMESTONE, a Trade Journal Published by Limestone Association of Japan: Mita business review, Keio University,47,115138,2004.

Simoni, M., Wilkes, M. D., Brown, S., Provis, J. L., Kinoshita, H., and Hanein, T.: Decarbonising the lime industry: State-of-the-art, Renew. Sustain. Energy Rev., 168, 112765, https://doi.org/10.1016/j.rser.2022.112765 , 2022.

Spring, C. R. and Cirella, G. T.: Fostering Sustainable Development: Green Energy Policy in the European Union and the United States, in: Human Settlements, edited by: Cirella, G. T., Springer Singapore, Singapore, 101–137, https://doi.org/10.1007/978-981-16-4031-5_7 , 2022.

United States Geological Survey (USGS): Lime Statistics and Information | U.S. Geological

https://doi.org/10.5194/essd-2026-218
Preprint. Discussion started: 22 April 2026

Survey: https://www.usgs.gov/centers/national-minerals-information-center/lime-statistics-and-information (last access: 18 January 2026), 2026a.

United States Geological Survey (USGS): Iron and Steel Slag Statistics and Information | U.S. Geological Survey: https://www.usgs.gov/centers/national-minerals-information-center/iron-and-steel-slag-statistics-and-information (last access: 18 January 2026), 2026b.

United States Geological Survey (USGS): Bauxite and Alumina Statistics and Information | U.S. Geological Survey: https://www.usgs.gov/centers/national-minerals-information-center/bauxite-and-alumina-statistics-and-information (last access: 18 January 2026), 2026c.

United Nations Department of Economic and Social Affairs Statistical Yearbook(UNSDW) : https://unstats.un.org/UNSDWebsite/Publications/StatisticalYearbook/ (last access: 18 January 2026), 2026.

United Nations Human Settlements Programme (UN-Habitat): World Cities Report 2022: Envisaging the Future of Cities, Nairobi, UN-Habitat, 2022, 422 pp., available at: https://unhabitat.org/wcr/2022 (last access: 18 January 2026), 2026.

Upravlenie S. U. T. statisticheskoe: National economy of the USSR: statistical yearbook, U.S. Joint Publications Research Service, Washington, DC, USA, 866 pp., 1961.

Wang Q-L, Shen F-C, Luo M-Z, et al. Progress and Application of Calcium Carbonate Produced by Precipitation Method[J]. Materials Science and Engineering,20(2):306-312. https://doi.org/10.3969/j.issn.1673 , 2002

Wu, S., Shao, Z., Andrew, R. M., Bing, L., Wang, J., Niu, L., Liu, Z., and Xi, F.: Global CO2 uptake by cement materials accounts 1930–2023, Sci. Data, 11, 1409, https://doi.org/10.1038/s41597-024-04234-8, 2024.

Xi, F., Davis, S. J., Ciais, P., Crawford-Brown, D., Guan, D., Pade, C., Shi, T., Syddall, M., Lv, J., and Ji, L.: Substantial global carbon uptake by cement carbonation, Nat. Geosci., 9, 880–883, https://doi.org/10.1038/NGEO2840, 2016.

Yang, Y., Xu, W., Wang, Y., Shen, J., Wang, Y., Geng, Z., Wang, Q., and Zhu, T.: Progress of CCUS technology in the iron and steel industry and the suggestion of the integrated application schemes for China, Chem. Eng. J., 450, 138438, https://doi.org/10.1016/j.cej.2022.138438, 2022.

Yang, Y., Holappa, L., Saxen, H., and van der Stel, J.: Ironmaking, in: Treatise on process metallurgy, Elsevier, 7–88, https://doi.org/10.1016/B978-0-323-85373-6.00017-1, 2024.

Yi, H., Xu, G., Cheng, H., Wang, J., Wan, Y., and Chen, H.: An overview of utilization of steel

https://doi.org/10.5194/essd-2026-218
Preprint. Discussion started: 22 April 2026

914 slag, Procedia Environ. Sci., 16, 791–801, https://doi.org/10.1016/j.proenv.2012.10.108, 2012.

915 Zementwerke eV, V. D.: Environmental Data of the German Cement Industry 2008,
916 https://mitglieder.vdzonline.de/fileadmin/gruppen/vdz/3LiteraturRecherche/UmweltundResso
917 urcen/Umweltdaten/Umweltdaten2007_e_Final_WEB.pdf , 2021.

918 Zhao, Q., Liu, C., Mei, X., Saxén, H., and Zevenhoven, R.: Research progress of steel slag-
919 based carbon sequestration, Fundam. Res., 5, 282–287,
920 https://doi.org/10.1016/j.fmre.2022.09.023, 2025.